https://doi.org/10.5194/egusphere-2026-3276
Preprint. Discussion started: 24 June 2026


# SWOT fast-sampling observations of topographically modulated coastal-eddy propagation in the Algerian Basin

Martina Auditore[1], Baptiste Mourre[2], and Paolo Oddo[1]

[1]Department of Physics and Astronomy, University of Bologna, Bologna, Italy
[2]Mediterranean Institute for Advanced Studies, IMEDEA (CSIC-UIB), Esporles, Spain

**Correspondence:** Baptiste Mourre (bmourre@imedea.uib-csic.es)

**Abstract.** The detailed evolution of coastal mesoscale eddies propagating along continental margins is difficult to observe with conventional nadir altimetry due to the limited spatio-temporal sampling. Here we use observations from the one-day repeat fast-sampling phase of the high-spatial-resolution Surface Water and Ocean Topography (SWOT) mission to examine the propagation of a small anticyclonic coastal eddy along the Algerian Coast in the Western Mediterranean Sea in May–June 2023. SWOT sea level anomaly fields are compared with conventional altimetry, sea surface temperature, and chlorophyll-a observations to assess the eddy position, structure, and evolution. SWOT resolves a more realistic nearshore eddy structure, leading to an improved characterization of its eastward displacement compared to conventional gridded altimetry, particularly during the eddy interaction with capes and steep bathymetric transitions. Ellipse-based centroid tracking indicates localized apparent propagation-speed maxima of about 20 cm $s^{-1}$, whereas conventional gridded altimetry produces smoother and weaker velocities, generally below 10 cm $s^{-1}$. These speed maxima coincide with a narrowing continental shelf and sharper shelf-break slopes, suggesting kinematic variability organized by the local coastal topography. This case study demonstrates the value of SWOT fast-sampling observations for resolving coastal eddy deformation and event-scale kinematic variability, highlighting new opportunities for understanding the interaction between small mesoscale eddies and coastal topography.

## 1 Introduction

Coastal mesoscale eddies influence alongshore transports and cross-shelf exchanges, key mechanisms for the transport of nutrients, heat, and mass between coastal and open-ocean environments (Akpınar et al., 2020, Manso-Narvarte et al. 2021, Combes et al., 2013). They transport nutrient-rich waters, enhancing primary productivity and shaping plankton distribution (Peliz et al., 2004; Brzezinski et al., 2011). They also contribute to kinetic energy transfers, influencing upper-ocean energy balance and mixing processes (Torres et al., 2023). Coastal eddies are generated by different processes, including interactions between coastal currents and topographic features, barotropic and baroclinic instabilities, and wind-driven dynamics (Pares-Sierra et al., 1993; Millot, 1999; Djakouré et al., 2014; Poulain et al., 2021). Influenced by shelf advection, topographic constraints and Rossby or coastal-trapped waves, they can then propagate along the coast. Examples have been reported in several areas, including Bay of Bengal (Mandal et al., 2019), Gulf of Aden (Al Saafani et al., 2007), east Australian coast (Everett et al., 2012; Archer et al., 2017), Gulf of Guinea (Djakouré et al., 2014), Mozambique Channel (Schouten et al.,

https://doi.org/10.5194/egusphere-2026-3276
Preprint. Discussion started: 24 June 2026


2003), Southern California Bight (DiGiacomo and Holt, 2001), straits of Florida (Parks et al., 2009), Brazil continental margin (Uchoa et al., 2023), Algerian basin (Escudier et al., 2016) or South China Sea (Chen et al., 2011).

In particular, the Algerian basin (Figure 1) is a recognized area for the formation, alongshore propagation and offshore detachment of coastal eddies (Font et al., 1998; Millot 1999; Obaton et al., 2000; Puillat et al. 2002, Escudier et al., 2016; Pessini et al., 2018). Surface circulation is dominated by the eastward-flowing Algerian Current, transporting relatively fresh Atlantic Water entering through the Strait of Gibraltar (Pinardi and Masetti, 2000). Baroclinic instabilities associated with this current generate cyclonic and anticyclonic mesoscale eddies, called Algerian Eddies (AEs). Figure 1 shows their typical propagation pathways, shaped by interactions with the Western and Eastern Algerian Gyres (Testor et al., 2005; Mallil et al., 2022). These features constrain eddy trajectories either along the continental slope or toward the basin interior (Escudier et al., 2016). Analysis of 20 years of satellite altimeter measurements estimated an average propagation speed of 3 cm/s for coastal eddies along the African coast (Escudier et al., 2016).

Mesoscale eddies propagating along continental slopes are dynamically constrained by topography. Through potential vorticity conservation, bathymetry variations can steer eddy motion and influence their pathways along continental margins. Theoretical and numerical studies have investigated these processes (Smith and O'Brien, 1983; Jacob et al., 2002; An and Mc Donald, 2005; van Heijst and Clercx, 2009; Rypina et al., 2020; Zhao et al., 2025). Using numerical simulations, Sutyrin et al. (2003) analyzed the interaction between baroclinic eddies and continental slopes, showing that eddy propagation near coastal boundaries depends on several factors including the $\beta$-effect, lower-layer circulation, shelf width and depth, and slope characteristics. Their results highlighted the modification of the lower-layer flow by the vortex-slope interaction, with an important role of the relative scale between eddy radius and shelf width in determining eddy propagation.

However, direct observational evidence of topographically controlled propagation in coastal areas remains limited and resolving spatial variability near continental margins has been challenging. High-Frequency radars provide valuable insights but are restricted to localized regions (e.g. Parks et al. 2009; Kim, 2010; Kirincich, 2016; Archer et al., 2017; Lai et al., 2017; Mandal et al., 2019). Satellite observations face various limitations. On the one hand, high-resolution satellite Sea Surface Temperature (SST) and Ocean Color (OC) provide valuable measurements but are sensitive to cloud presence. On the other hand, conventional altimetry products have limited spatio-temporal resolution. While the nominal along-track resolution depends on the sampling frequency, typically 6-7 km at 1Hz, approximately 1 km at 5 Hz (Pujol et al., 2022), this sampling capability is not reflected in mapped sea level anomaly fields derived from interpolation, whose spatial resolution is typically limited to eddies with radius larger than 50 km at midlatitudes (Ballarota et al., 2019). Moreover, conventional altimeter measurements face specific limitations approaching the coast due to land contamination of radar and radiometer signals, which, combined with a complex coastal tidal dynamics, reduces the accuracy of the sea surface elevation estimates and associated atmospheric and tidal geophysical corrections (Vignudelli et al., 2011).

The Surface Water and Ocean Topography (SWOT) mission, launched in December 2022, provides new monitoring capabilities which overcome some of these limitations. Using Ka-band Radar Interferometry (KaRIn), it measures sea surface height across a 120-km swath, providing the first-ever direct synoptic observations of ocean topography in two dimensions (Morrow et al., 2019; Fu et al., 2024). The increased resolution (250m and 2km for gridded products over the ocean) provides details

https://doi.org/10.5194/egusphere-2026-3276
Preprint. Discussion started: 24 June 2026


of the variability of the sea surface elevation down to wavelengths of 5 km (Fu et al., 2024), with observations much closer to the coast compared to conventional along-track altimetry. Despite potential persistent small-scale uncertainties in geophysical corrections (Hay et al., 2025), SWOT offers a new high-resolution all-weather monitoring of coastal regions. SWOT was shown to improve the detection of ocean fronts and small and coastal mesoscale eddies (Archer et al., 2025, Verger-Miralles et al., 2025; Coadou-Chaventon et al., 2025; Fortunato et al., 2025, Wang et al., 2025), as well as storm surges footprints in coastal areas (Vega-Gimenez et al., 2025). During its initial fast-sampling phase (March–July 2023), SWOT operated in a 1 day-repeat orbit, enabling high-frequency observations over specific regions. This unprecedented combination of spatial and temporal coverage offers a unique opportunity to resolve coastal eddies and investigate their dynamics. In this context, this study uses SWOT observations during its fast-sampling phase to investigate how topographic interactions affect the evolution of a coastal mesoscale eddy in the Algerian Basin, thereby providing observational insight into eddy–topography interactions predicted by theory. The central question addressed here is not only whether SWOT is able to resolve a specific coastal eddy, but whether wide-swath altimetry can reveal short-lived kinematic changes and deformations of such eddies which observation is limited by conventional nadir altimetry. We use this coastal Algerian eddy as a test case for a broader observational problem: how to characterize eddy motion near continental margins when topographic steering, deformation, and limited sampling occur on comparable spatial and temporal scales.

Section 2 describes datasets and methodology used to identify and track the coastal eddy. Section 3 presents the results of eddy detection and alongshore propagation analysis. Finally, Section 4 discusses and summarizes the main findings.

## 2 Data and methods

The first dataset used in this study consists of Sea Level Anomaly (SLA) observations from SWOT mission. We employed the Level 3 product (version 2.0.1, AVISO+) from the initial fast-sampling phase, which provides SLA two-dimensional fields with a nominal spatial resolution of 2 km. Additionally, conventional altimetry products from the Copernicus Marine Service were used. These included both Level 3 along-track and Level 4 gridded SLA data. The L4 product provides daily SLA on a 1/16° regular grid and is derived from optimal merging of data from multiple satellite altimeters. The L3 product along-track resolution is ∼7 km. SST and OC data were used to qualitatively assess surface signatures associated with the observed eddy. For SST, the analysis relied on the L3 SST product for the Mediterranean Sea (Buongiorno Nardelli et al., 2013). This dataset provides daily maps at high spatial resolution ( 1 km), representative of the foundation temperature (free from diurnal cycle). Chlorophyll-a concentration (CHL-a), derived from ocean-color observations, provides daily fields at 1 km resolution and was used as a tracer of surface water-mass contrasts. Both SST and OC data were downloaded from Copernicus Marine Service.

The eddy tracking was performed using two different approaches, depending on the SLA dataset. For the conventional altimetry gridded fields, eddies were detected using the PyEddyTracker algorithm (PET, Mason et al., 2014). PET identifies eddy structures as closed contours of SLA satisfying a minimum amplitude and size threshold. For the SWOT data, a custom procedure was required due to the higher resolution and noisier nature of the L3 SWOT fields. Recent studies have applied PET directly to native SWOT swath data by reconstructing the nadir gap through inpainting techniques before contour extraction (de

https://doi.org/10.5194/egusphere-2026-3276
Preprint. Discussion started: 24 June 2026


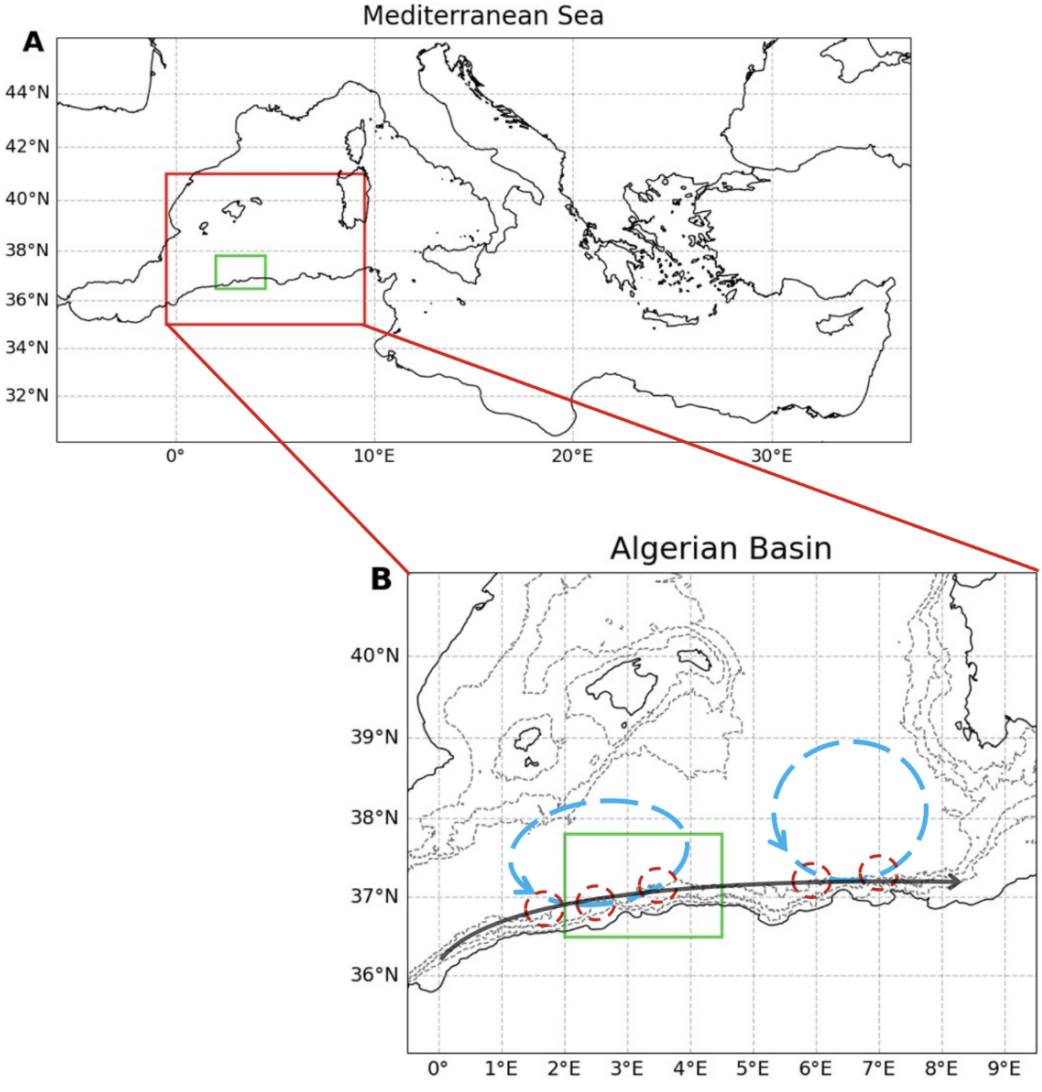


**Figure 1.** Panel A: Mediterranean Sea, the red rectangle indicates the Algerian Basin. Panel B: Algerian Basin with: Algerian Current (black arrow) and Western/Eastern Algerian Gyres (blue dashed arrows), which drive the propagation of coastal mesoscale eddies (red dashed lines). The green rectangle represents the study area.

https://doi.org/10.5194/egusphere-2026-3276
Preprint. Discussion started: 24 June 2026


Marez et al. 2026). In the present work, we adopted a different strategy based on geometric reconstruction of the eddy shape. First, SLA maps were low-pass filtered using a second-order Butterworth filter with a cutoff wavelength of approximately 33 km, in order to reduce small-scale noise while preserving mesoscale structures. Eddy contours were then extracted by selecting points within a tolerance of $\pm 0.005$ m around a chosen SLA level representative of the eddy boundary. Because the resulting contours were often incomplete, the eddy boundary was first reconstructed and then fitted with an ellipse using a least-squares approach, providing a simplified representation of eddy geometry. This approximation was particularly useful during phases of eddy deformation or topographic interaction, where raw contours became noisy or discontinuous. The eddy apparent alongshore speed was computed by tracking the displacement of the eddy centroid over time. For conventional altimetry, centroid positions were provided directly by PET. For SWOT data, the center of the fitted ellipse was used as a proxy for the eddy centroid. The fitted ellipse should therefore be interpreted as a compact geometric descriptor of the SLA anomaly, not as a material eddy boundary. The resulting speed estimates describe the displacement of this fitted structure and may include contributions from translation, deformation, and partial sampling.

## 3 Results

### 3.1 Altimeter data evaluation against independent satellite tracer fields

Figure 2 presents a qualitative comparison between SLA derived from SWOT and from conventional altimetry, overlaid on independent tracer fields. These tracers (SST and CHL-a) serve as qualitative references, offering a validation for the positioning and shape of eddy features. On both dates, SWOT's SLA shows a very good correspondence with the observed tracers. On 15 May (Fig. 2a), SWOT SLA contours closely follow the thermal gradients, clearly delineating a coastal eddy centered around 37°N 2.5°E. Conventional altimetry, however, shows a slightly displaced feature with limited detail near the coast. A similar improvement is seen in the chlorophyll-a fields from 4 June (Fig. 2b), after the eddy has propagated and elongated along the coast. SWOT more clearly identifies small-scale features, particularly near the continental slope, providing SLA contours consistent with CHL-a gradients. Overall, this comparison highlights SWOT's improved capability in detecting both mesoscale and smaller-scale coastal structures.

### 3.2 Evolution of the coastal eddy

We now examine the evolution of the coastal eddy captured by both conventional altimetry and SWOT. This anticyclonic structure was first identified in early May and remained visible for nearly six weeks in multiple fields (SLA, SST, CHL-a), all showing an eastward propagation along the continental slope. Figure 3 shows the eddy SLA evolution in both conventional altimetry and SWOT. In all panels, the black contours correspond to the maximum SLA in the center of the eddy minus a constant value of 3.5 cm. This criterion allows us to highlight SLA gradients: the smaller the eddy contour, the more intense the SLA gradients and associated geostrophic velocities. The eddy structure is identifiable in conventional gridded altimetry fields over the whole period. The eddy slightly loses intensity on 26 May, shown by a reduction in SLA amplitude (Fig.

https://doi.org/10.5194/egusphere-2026-3276
Preprint. Discussion started: 24 June 2026


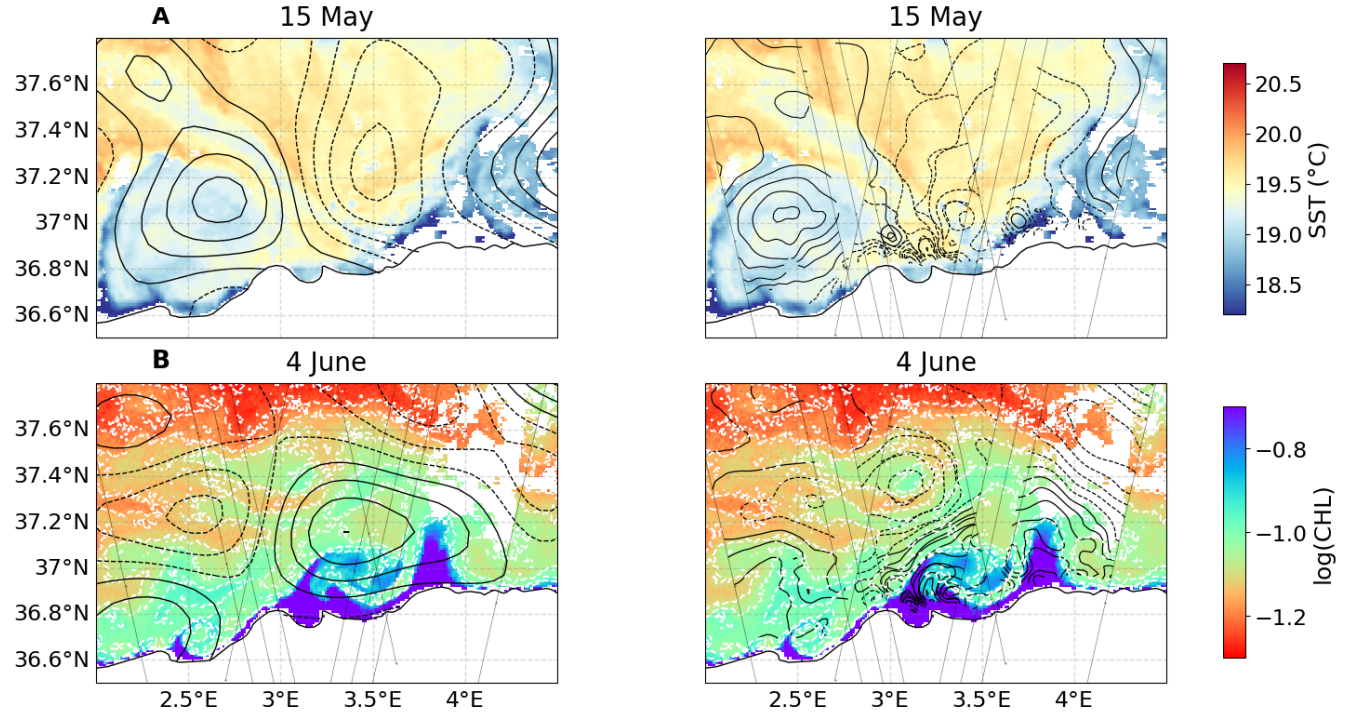


**Figure 2.** Comparison of SLA fields derived from conventional gridded altimetry (left) and SWOT (right), overlaid on independent satellite tracer observations: (A) SST (15 May); (B) CHL-a (4 June). Black lines represent the SLA at 1.5 cm intervals (solid positive, dashed negative). White dashed lines represent CHL-a levels (every 0.06), while color maps represent the tracer fields. SWOT data ©NASA / CNES.

3c), before elongating in early June (Fig. 3e). Five days later, the eddy SLA magnitude increases again, and the eddy regains a circular shape (Fig. 3f). SWOT SLA maps depict the eddy with greater spatial definition and structural detail. Notably, the eddy contour appears smaller in SWOT than in conventional altimetry, indicating larger SLA gradients and associated geostrophic velocities. Initially (Fig. 3g, 3h), the eddy exhibits a well-defined close-to-circular anticyclonic pattern with a strong positive SLA core. The eddy then translates eastwards. Similarly to conventional altimetry, it slightly loses intensity on 26 May. The eddy then approaches the coast (Fig 3j), while it progressively deforms. The eddy regains intensity around 31 May-5 June (Fig. 3j, 3k), with a shape becoming elongated and asymmetric as it continues propagating eastwards (Fig. 3l). This comparison highlights a clear difference in the representation of eddy propagation and deformation with respect to conventional gridded altimetry. While both datasets capture the general eastward trajectory, SWOT provides a more detailed representation of the evolution of the position and shape of the eddy.

These differences highlight the spatio-temporal resolution limitations in conventional altimetry, which are overcome with SWOT observations. Figure 4 shows the distribution of available altimeter along-track observations during a 20-day window centered on 26 May. It shows that there are no measurements crossing the eddy on that day nor on the days just before or

https://doi.org/10.5194/egusphere-2026-3276
Preprint. Discussion started: 24 June 2026


after. This temporal and spatial sparsity compromises interpolation, leading to an approximate representation of the eddy in the gridded L4 maps.

### 3.3 Alongshore propagation and interaction with topography

The high spatio-temporal resolution provided by SWOT observations allows us to characterize the details of the alongshore propagation of the eddy. Figure 5A shows the evolution of the position and ellipse-fitted shape of the eddy from 8 May to 12 June. From 8 to 25 May, the eddy propagates eastward approximately parallel to the coastline. Around 29 May, near the longitude of Cape Caxine ( 3°E), the eddy approaches the coast, likely in response to an interaction with the continental slope. During this period the eddy becomes strongly elongated, indicating a substantial deformation of its structure. Between 31 May and 4 June the eddy lies very close to the coastline. Following this phase, the eddy weakens and progressively moves away from the coast while continuing its eastward propagation with reduced intensity. This behavior suggests that the eddy evolution is strongly influenced by coastal topography.

The eddy's centroid displacement speed is analyzed in Figure 5B, comparing daily speeds from conventional altimetry and SWOT. SWOT velocities show greater amplitude and day-to-day variability. Peaks with propagation velocities above or around 20 cm/s around 24 May and 1 June are captured by SWOT, while the estimates from conventional altimetry remain below 10 cm/s. The two main velocity peaks (around 2.95°E and 3.25°E) correspond to areas close to specific coastal capes (Capes Caxine and Matifou), with increased bathymetric gradients. Conventional altimetry shows an overall smoother and lower velocity profile, failing to capture these two periods of localized accelerations. These results suggest that SWOT more effectively captures the structural evolution and kinematic variability of the eddy during its interaction with topography.

To investigate the role of bathymetry, propagation velocities are color-coded by the distance of the coast to the 200 m isobath, used as a proxy for continental shelf width. In this area, it is also in good correspondence with the shelf break steepness, where the bottom depth increases to more than 2000m over a few kilometers (represented by circle size in Figure 5B). The two main centroid-based propagation speed peaks correspond to both a narrowing of the continental shelf and an increase of the bathymetric slope, associated with the two capes mentioned above. Around 24 May (2.9-3.0°E), eddy propagation reaches its maximum speed (21.7cm/s) where the 200m isobath is very close to the coast with a sharp slope of the continental shelf break. In the following days (24–27 May), its propagation velocity decreases as this distance increases again, until approaching the next Cape on 30 May. The spatial correspondence between centroid-speed maxima and steep bathymetric transitions suggests that the kinematic variability resolved by SWOT is organized relative to the local shelf geometry. However, this correspondence should not be interpreted as a complete dynamical diagnosis. During this phase, the eddy is strongly deformed and only partially described by the fitted ellipse, so the estimated velocities include contributions from both translation and changes in eddy shape. The localized speed maxima observed near Capes Caxine and Matifou are therefore interpreted as kinematic signatures consistent with topographic modulation, rather than as direct evidence of a closed dynamical balance. This interpretation is compatible with theoretical and numerical studies of eddy–slope interaction, which show that continental slopes and coastal boundaries can influence eddy trajectories and structure through mechanisms involving the $\beta$-effect, lower-layer flow

https://doi.org/10.5194/egusphere-2026-3276
Preprint. Discussion started: 24 June 2026


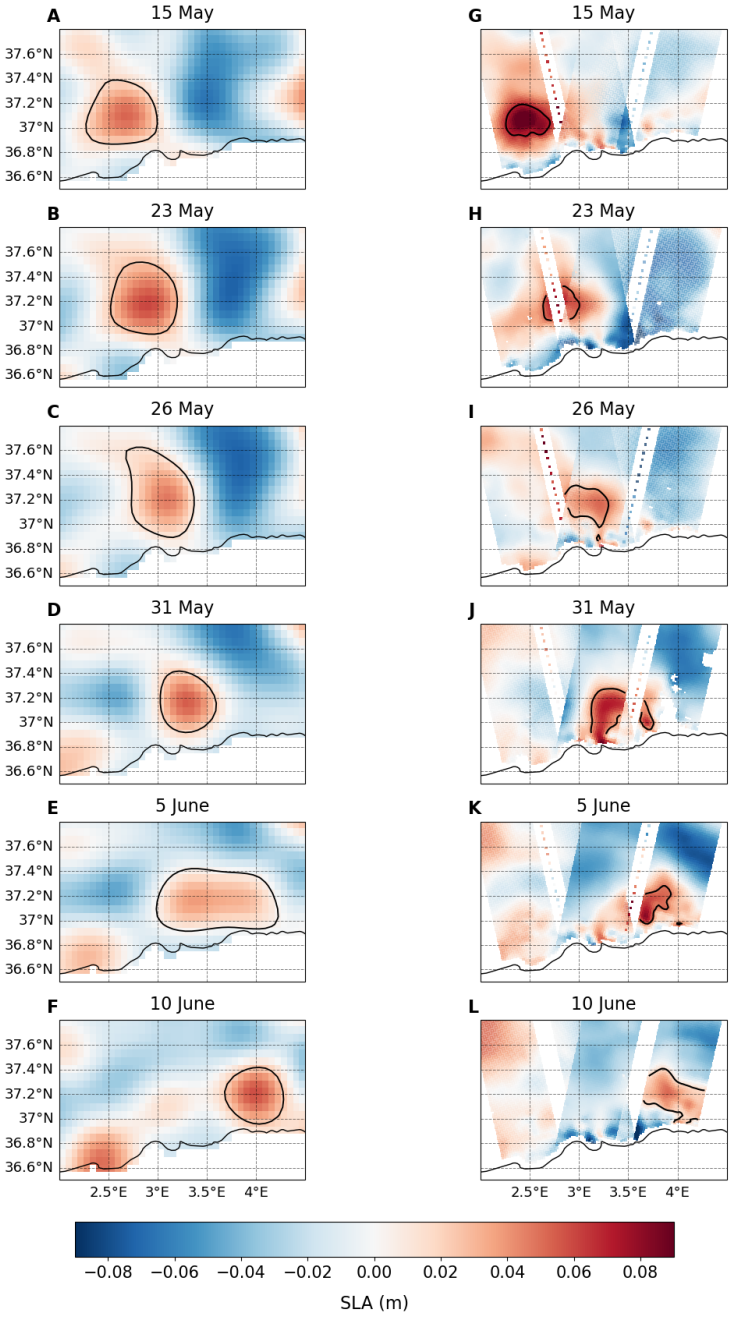


**Figure 3.** Evolution of the coastal eddy along the Algerian coast from 15 May to 10 June, 2023, according to: 1) conventional gridded altimetry (panels A to F), and 2) SWOT (panels G to L). The sequence illustrates the eastward propagation and deformation of the eddy structure during the study period. The black contours represent an isoline with a value defined as the maximum SLA in the eddy center minus a constant value of 3.5 cm. SWOT data ©NASA / CNES.

https://doi.org/10.5194/egusphere-2026-3276
Preprint. Discussion started: 24 June 2026


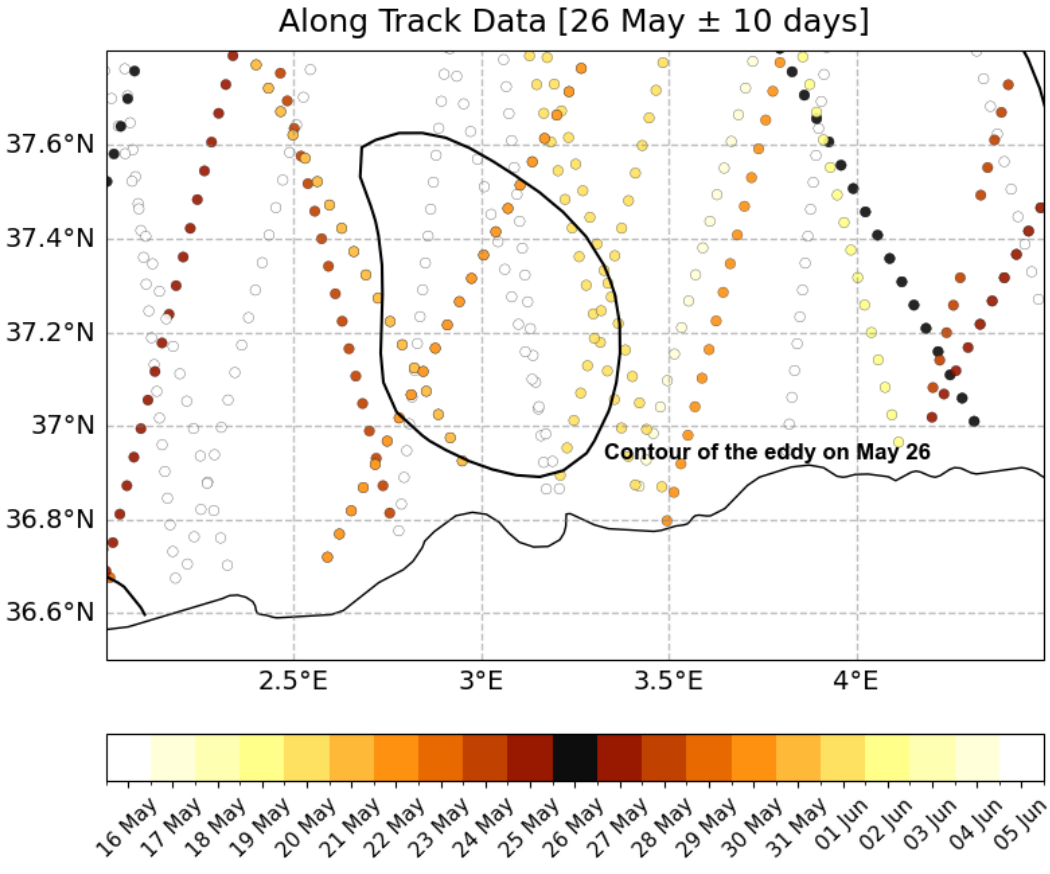


**Figure 4.** Spatial distribution of conventional altimeter along-track data within a 20-day window centered on 26 May. The colorbar indicates the absolute difference in days from 26 May, the black contour outlines the eddy identified on that date.

adjustments, and changes in shelf geometry (Sutyrin et al., 2003). The results presented here thus highlight fine-scale kinematic variability associated with coastal topography that is largely smoothed in conventional gridded altimetry products.

## 4 Discussion and conclusions

This study documents the detailed alongshore propagation of a coastal mesoscale eddy in the Algerian Basin during the SWOT fast-sampling phase. The high-resolution, two-dimensional observations provided by SWOT allow a refined description of eddy trajectory, deformation, and propagation speed, which variability appears to be modulated by coastal topography.

The spatial structure of the eddy captured from SWOT showed a close agreement with independent tracers (SST and CHL-a), especially near the coast, and revealed fine-scale features absent in gridded altimetry products. The analysis of the propagation speed of the eddy using SWOT observations resulted in significantly higher and more variable velocities compared to conventional altimetry, highlighting in particular acceleration phases when approaching specific capes where the continental

https://doi.org/10.5194/egusphere-2026-3276
Preprint. Discussion started: 24 June 2026


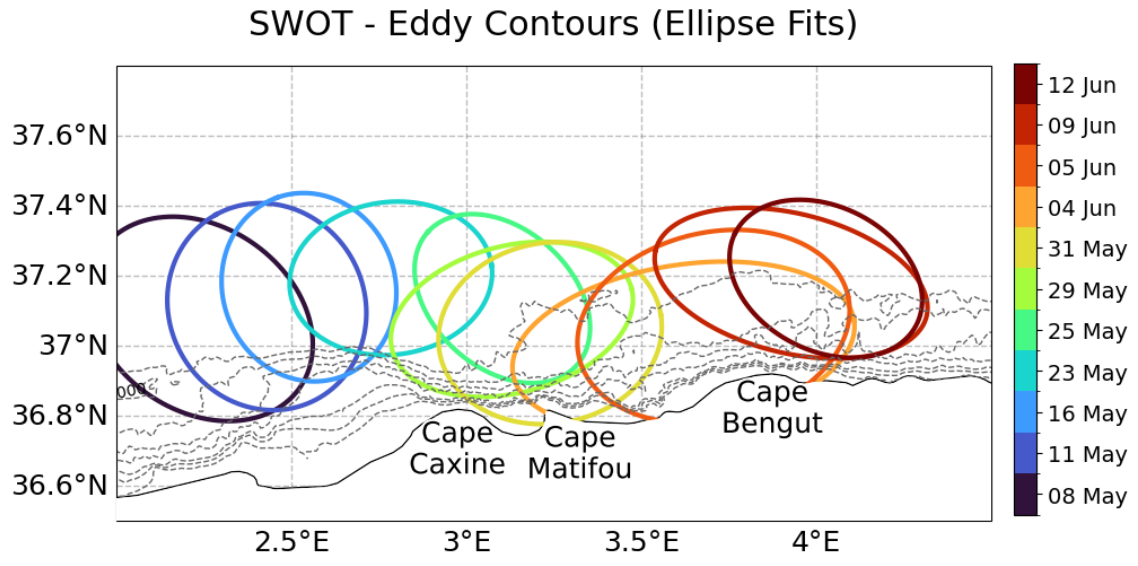


**Figure 5.** Ellipse-fitted sea level anomaly contours associated with the coastal eddy between 8 May and 12 June, 2023. Contours are color-coded by date. Grey dashed lines indicate bathymetric contours.

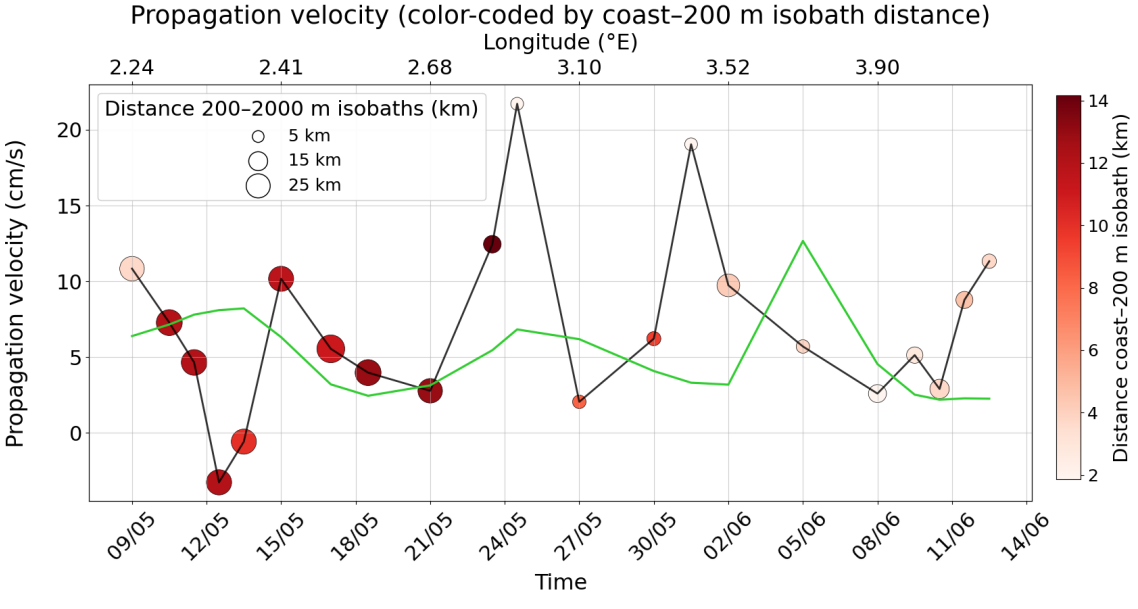


**Figure 6.** Time series of the eddy alongshore propagation velocity (cm/s) derived from SWOT (black) and from conventional altimetry (green). In the SWOT time series, circles indicate two key features of the coastal topography. While the color of the circles represents the distance from the coast to the 200m isobath (as a proxy for width of the continental shelf), their size is proportional to the distance between the 200m and 2000m isobaths (as a proxy for shelf-break steepness).

https://doi.org/10.5194/egusphere-2026-3276
Preprint. Discussion started: 24 June 2026


shelf gets thinner and the shelf break slope sharper. The observed behavior suggests a dynamical influence of bathymetry on eddy propagation along the continental margin, consistent with theoretical studies of eddy–slope interaction. The present results provide an observational perspective on these processes in a real coastal environment, highlighting localized kinematic adjustments that are largely smoothed in conventional gridded altimetry products. SWOT measurements offer a new potential to better understand eddy-topography interactions. Appropriate vorticity balances and advection analysis could then be carried out to unravel the mechanisms driving these interactions.

Note that the fast-sampling was limited to the initial three months of the mission and was limited to selected tracks. This high-frequency sampling enabled the detailed analysis of coastal eddy propagation presented here. Moreover, uncertainties related to coastal geophysical corrections were probably weak due to the low tidal signal and relatively dry weather of our study case. During the nominal repeat orbit, SWOT alone cannot provide the daily temporal sampling required to reconstruct comparable event-scale deformation and centroid-speed variability. Similar studies during the nominal phase will generally require synergy with conventional altimetry, SST, ocean color, in situ observations, coastal radar where available, or model/data-assimilation products. Nevertheless, analyses like this one can help build confidence in SWOT measurements and improve our understanding of the spatial and temporal scales that can be resolved, particularly for ocean state estimation and data assimilation systems, for which representing mesoscale variability and coastal dynamics remains challenging.

The partial coverage of the eddy by SWOT data did not allow us to successfully apply conventional eddy-tracking algorithms. This led us to use an approach based on ellipse fitting to characterize the propagation speed of the eddy. While recent studies (de Marez et al., 2026) based on SWOT have relied on gap-filling strategies, such as biharmonic inpainting, to reconstruct continuous SLA fields prior to applying standard eddy detection and tracking algorithms, our approach instead preserves the native structure of the observed anomaly and represents it through a simplified geometric approximation. This approach might have limitations in case of strong distortions of the structure and more advanced analysis methods could be developed to better reflect the real irregular deformation of the eddy, especially during its interaction with topography. This could result in an improvement of the accuracy of propagation speed estimates, also allowing to distinguish between deformation and translation effects.

Despite these limitations, the case illustrates how SWOT fast-sampling observations can complement conventional gridded altimetry in coastal regions by resolving eddy deformation, nearshore structure, and short-lived kinematic variability that are otherwise strongly smoothed. The broader contribution of this study is therefore not a complete dynamical diagnosis of one Algerian eddy, but an observational demonstration of what wide-swath altimetry can and cannot resolve during coastal eddy–topography interactions. This provides a useful benchmark for future studies combining SWOT with complementary observations and models to investigate topographically influenced mesoscale dynamics along continental margins.

*Code and data availability.* All the datasets used in this study are publicly accessible and listed here.

- The SWOT Level-3 KaRIn Low Rate SSH Expert data (v2.0.1): https://doi.org/10.24400/527896/A01-2023.018.

https://doi.org/10.5194/egusphere-2026-3276
Preprint. Discussion started: 24 June 2026


- European Seas Gridded L4 Sea Surface Heights And Derived Variables Reprocessed 1993 Ongoing: https://doi.org/10.48670/moi-00141.
- European Seas Along Track L 3 Sea Surface Heights Reprocessed 1993 Ongoing Tailored For Data Assimilation: https://doi.org/10.48670/moi-00139.
- Mediterranean Sea - High Resolution and Ultra High Resolution L3S Sea Surface Temperature Reprocessed: https://doi.org/10.48670/moi-00314.
- Mediterranean Sea, Bio-Geo-Chemical, L3, daily Satellite Observations: https://doi.org/10.48670/moi-00297.

The main codes used in this study are available on Zenodo (Auditore, 2026).

*Author contributions.* M.A.: Investigation, Formal analysis, Visualization, Writing – original draft, Writing – review & editing. B.M. And P.O.: Conceptualization, Methodology, Supervision, Writing – original draft, Writing – review & editing. All authors approved the final version of the manuscript.

*Competing interests.* The authors declare there are no conflicts of interest for this manuscript.

*Acknowledgements.* The authors acknowledge funding from the Spanish Ministry of Science, Innovation, and Universities (MICIU), the Spanish Research Agency (AEI) and the European Regional Development Fund through the grant PID2021-122417NB-I00 (FaSt-SWOT project, MCIN/AEI/10.13039/501100011033/FUE/). Additional support came from the SWINT project (CNS2023-145542 by MCIN/AEI/10.13039/501100011033/ NextGenerationEU/PRTR). Part of the work was conducted at IMEDEA, a María de Maeztu Centre of Excellence supported by AEI/MICIU (CEX2021-001198). The authors acknowledge useful discussions with the members of the Physical Oceanography and Climate group at IMEDEA, in particular Ananda Pascual, Elisabet Verger-Miralles and Laura Gómez-Navarro.

https://doi.org/10.5194/egusphere-2026-3276
Preprint. Discussion started: 24 June 2026


## References

Akpınar, A., Charria, G., Theetten, S., and Vandermeirsch, F.: Cross-shelf exchanges in the northern Bay of Biscay, J. Mar. Syst., 205, 103314, https://doi.org/10.1016/j.jmarsys.2020.103314, 2020.

Al Saafani, M. A., Shenoi, S. S. C., Shankar, D., Aparna, M., Kurian, J., Durand, F., and Vinayachandran, P. N.: Westward movement of eddies into the Gulf of Aden from the Arabian Sea, J. Geophys. Res.-Oceans, 112, C11004, https://doi.org/10.1029/2006JC004020, 2007.

An, B. and McDonald, N. R.: Coastal currents and eddies and their interaction with topography, Dyn. Atmos. Oceans, 40, 237–253, https://doi.org/10.1016/j.dynatmoce.2005.04.002, 2005.

Archer, M. R., Roughan, M., Keating, S. R., and Schaeffer, A.: On the variability of the East Australian Current: Jet structure, meandering, and influence on shelf circulation, J. Geophys. Res.-Oceans, 122, 8464–8481, https://doi.org/10.1002/2017JC013097, 2017.

Archer, M., Wang, J., Klein, P., Dibarboure, G., and Fu, L.-L.: Wide-swath satellite altimetry unveils global submesoscale ocean dynamics, Nature, 640, 691–696, https://doi.org/10.1038/s41586-025-08722-8, 2025.

Auditore, M.: Codes to accompany "SWOT fast-sampling observations of topographically modulated coastal-eddy propagation in the Algerian Basin" (v1) [code], Zenodo, https://doi.org/10.5281/zenodo.20445357, 2026.

AVISO/DUACS: SWOT Level-3 KaRIn Low Rate SSH Expert (v2.0.1) [Dataset], CNES [dataset], https://doi.org/10.24400/527896/A01-2023.018, 2024.

Ballarotta, M., Ubelmann, C., Pujol, M.-I., Taburet, G., Fournier, F., Legeais, J.-F., Faugère, Y., Delepoulle, A., Chelton, D., Dibarboure, G., and Picot, N.: On the resolutions of ocean altimetry maps, Ocean Sci., 15, 1091–1109, https://doi.org/10.5194/os-15-1091-2019, 2019.

Brzezinski, M. A. and Washburn, L.: Phytoplankton primary productivity in the Santa Barbara Channel: Effects of wind-driven upwelling and mesoscale eddies, J. Geophys. Res.-Oceans, 116, C12013, https://doi.org/10.1029/2011JC007397, 2011.

Chen, G., Hou, Y., and Chu, X.: Mesoscale eddies in the South China Sea: Mean properties, spatiotemporal variability, and impact on thermohaline structure, J. Geophys. Res.-Oceans, 116, C06018, https://doi.org/10.1029/2010JC006716, 2011.

Combes, V., Chenillat, F., Di Lorenzo, E., Rivière, P., Ohman, M. D., and Bograd, S. J.: Cross-shore transport variability in the California Current: Ekman upwelling vs. eddy dynamics, Prog. Oceanogr., 109, 78–89, https://doi.org/10.1016/j.pocean.2012.10.001, 2013.

Coadou-Chaventon, S., Swart, S., Novelli, G., and Speich, S.: Resolving sharper fronts of the Agulhas Current Retroflection using SWOT altimetry, Geophys. Res. Lett., 52, e2025GL115203, https://doi.org/10.1029/2025GL115203, 2025.

DiGiacomo, P. M. and Holt, B.: Satellite observations of small coastal ocean eddies in the Southern California Bight, J. Geophys. Res.-Oceans, 106, 22521–22543, https://doi.org/10.1029/2000JC000728, 2001.

Djakouré, S., Penven, P., Bourlès, B., Veitch, J., and Koné, V.: Coastally trapped eddies in the north of the Gulf of Guinea, J. Geophys. Res.-Oceans, 119, 6805–6819, https://doi.org/10.1002/2014JC010243, 2014.

Escudier, R., Mourre, B., Juza, M., and Tintoré, J.: Subsurface circulation and mesoscale variability in the Algerian subbasin from altimeter-derived eddy trajectories, J. Geophys. Res.-Oceans, 121, 6310–6322, https://doi.org/10.1002/2016JC011760, 2016.

CMEMS: E.U. Copernicus Marine Service Information, European Seas Gridded L4 Sea Surface Heights And Derived Variables Reprocessed 1993 Ongoing [Dataset], Marine Data Store (MDS), https://doi.org/10.48670/moi-00141, 2024.

CMEMS: E.U. Copernicus Marine Service Information, European Seas Along Track L3 Sea Level Anomalies Nrt [Dataset], Marine Data Store (MDS), https://doi.org/10.48670/moi-00140, 2024.

CMEMS: E.U. Copernicus Marine Service Information, Mediterranean Sea - High Resolution L3S Sea Surface Temperature Reprocessed [Dataset], Marine Data Store (MDS), https://doi.org/10.48670/moi-00314, 2024.

https://doi.org/10.5194/egusphere-2026-3276
Preprint. Discussion started: 24 June 2026


CMEMS: E.U. Copernicus Marine Service Information, Mediterranean Sea, Bio-Geo-Chemical, L3, daily Satellite Observations (Near Real Time) [Dataset], Marine Data Store (MDS), https://doi.org/10.48670/moi-00297, 2023.

Everett, J. D., Baird, M. E., Oke, P. R., and Suthers, I. M.: An avenue of eddies: Quantifying the biophysical properties of mesoscale eddies in the Tasman Sea, Geophys. Res. Lett., 39, L16608, https://doi.org/10.1029/2012GL053091, 2012.

Font, J., Isern-Fontanet, J., and De Jesus Salas, J.: Tracking a big anticyclonic eddy in the western Mediterranean Sea, Sci. Mar., 68, 331–342, https://doi.org/10.3989/scimar.2004.68n3331, 2004.

Fortunato, L., Gómez-Navarro, L., Combes, V., Cotroneo, Y., Aulicino, G., and Pascual, A.: Coastal Eddy Detection in the Balearic Sea: SWOT Capabilities, Remote Sens., 17, 2552, https://doi.org/10.3390/rs17152552, 2025.

Fu, L.-L., Pavelsky, T., Crétaux, J.-F., Morrow, R., Farrar, J. T., Vaze, P., Sengenes, P., Vinogradova-Shiffer, N., Sylvestre-Baron, A., Picot, N., and Dibarboure, G.: The Surface Water and Ocean Topography Mission: A Breakthrough in Radar Remote Sensing of the Ocean and Land Surface Water, Geophys. Res. Lett., 51, e2023GL107652, https://doi.org/10.1029/2023GL107652, 2024.

Hay, A., Watson, C., Legresy, B., King, M., and Beardsley, J.: Small scale variability in the wet troposphere impacts the interpretation of SWOT satellite observations, Geophys. Res. Lett., 52, e2024GL112778, https://doi.org/10.1029/2024GL112778, 2025.

van Heijst, G. J. F. and Clercx, H. J. H.: Laboratory modeling of geophysical vortices, Annu. Rev. Fluid Mech., 41, 143–164, https://doi.org/10.1146/annurev-fluid.010908.165207, 2009.

Kim, S. Y.: Observations of submesoscale eddies using high frequency radar-derived kinematic and dynamic quantities, Contin. Shelf Res., 30, 1639–1655, https://doi.org/10.1016/j.csr.2010.06.011, 2010.

Kirincich, A.: The occurrence, drivers, and implications of submesoscale eddies on the Martha's Vineyard inner shelf, J. Phys. Oceanogr., 46, 2645–2662, https://doi.org/10.1175/JPO-D-15-0191.1, 2016.

Lai, Y., Zhou, H., Yang, J., Zeng, Y., and Wen, B.: Submesoscale eddies in the Taiwan Strait observed by high-frequency radars: Detection algorithms and eddy properties, J. Atmos. Ocean. Technol., 34, 939–953, https://doi.org/10.1175/JTECH-D-16-0160.1, 2017.

Mallil, K., Testor, P., Bosse, A., Margirier, F., Houpert, L., Le Goff, H., Mortier, L., and Louanchi, F.: The Levantine Intermediate Water in the western Mediterranean and its interactions with the Algerian Gyres: Insights from 60 years of observation, Ocean Sci., 18, 937–952, https://doi.org/10.5194/os-18-937-2022, 2022.

Mandal, S., Sil, S., Pramanik, S., Arunraj, K. S., and Jena, B. K.: Characteristics and evolution of a coastal mesoscale eddy in the western Bay of Bengal monitored by high-frequency radars, Dyn. Atmos. Oceans, 88, 101107, https://doi.org/10.1016/j.dynatmoce.2019.101107, 2019.

Manso-Narvarte, I., Rubio, A., Jordà, G., Carpenter, J., Merckelbach, L., and Caballero, A.: Three-dimensional characterization of a coastal mode-water eddy from multiplatform observations and a data reconstruction method, Remote Sens., 13, 674, https://doi.org/10.3390/rs13040674, 2021.

de Marez, C., Bendinger, A., and Dilmahamod, A. F.: High-latitude eddy statistics from SWOT compared with in situ observations, Ocean Sci., 22, 1515–1528, https://doi.org/10.5194/os-22-1515-2026, 2026.

Mason, E., Pascual, A., and McWilliams, J. C.: A new sea surface height–based code for oceanic mesoscale eddy tracking, J. Atmos. Ocean. Technol., 31, 1181–1188, https://doi.org/10.1175/JTECH-D-14-00019.1, 2014.

Millot, C.: Circulation in the Western Mediterranean Sea, J. Mar. Syst., 20, 423–442, https://doi.org/10.1016/S0924-7963(98)00078-5, 1999.

Morrow, R., Fu, L.-L., Ardhuin, F., Benkiran, M., Chapron, B., Cosme, E., d'Ovidio, F., Farrar, J. T., Gille, S. T., Lapeyre, G., Le Traon, P.-Y., Pascual, A., Ponte, A., Qiu, B., Rascle, N., Ubelmann, C., Wang, J., and Zaron, E. D.: Global observations of

https://doi.org/10.5194/egusphere-2026-3276
Preprint. Discussion started: 24 June 2026


fine-scale ocean surface topography with the Surface Water and Ocean Topography (SWOT) mission, Front. Mar. Sci., 6, 232, https://doi.org/10.3389/fmars.2019.00232, 2019.

Obaton, D., Millot, C., Chabert D'Hières, G., and Taupier-Letage, I.: The Algerian current: Comparisons between in situ and laboratory data sets, Deep-Sea Res. Pt. I, 47, 2159–2190, https://doi.org/10.1016/S0967-0637(00)00014-5, 2000.

Pares-Sierra, A., White, W. B., and Tai, C.-K.: Wind-driven coastal generation of annual mesoscale eddy activity in the California Current, J. Phys. Oceanogr., 23, 1110–1122, https://doi.org/10.1175/1520-0485(1993)023<1110:WDCGOA>2.0.CO;2, 1993.

Parks, A. B., Shay, L. K., Johns, W. E., Martinez-Pedraja, J., and Gurgel, K.-W.: HF radar observations of small-scale surface current variability in the Straits of Florida, J. Geophys. Res.-Oceans, 114, C08002, https://doi.org/10.1029/2008JC005025, 2009.

Peliz, A., Santos, A. M. P., Oliveira, P. B., and Dubert, J.: Extreme cross-shelf transport induced by eddy interactions southwest of Iberia in winter 2001, Geophys. Res. Lett., 31, L08303, https://doi.org/10.1029/2004GL019618, 2004.

Pessini, F., Olita, A., Cotroneo, Y., and Perilli, A.: Mesoscale eddies in the Algerian Basin: Do they differ as a function of their formation site?, Ocean Sci., 14, 669–688, https://doi.org/10.5194/os-14-669-2018, 2018.

Pinardi, N. and Masetti, E.: Variability of the large scale general circulation of the Mediterranean Sea from observations and modelling: A review, Palaeogeogr. Palaeoclimatol. Palaeoecol., 158, 153–173, https://doi.org/10.1016/S0031-0182(00)00048-1, 2000.

Poulain, P.-M., Centurioni, L., Özgökmen, T., Tarry, D., Pascual, A., Ruiz, S., Mauri, E., Menna, M., and Notarstefano, G.: On the structure and kinematics of an Algerian eddy in the southwestern Mediterranean Sea, Remote Sens., 13, 3039, https://doi.org/10.3390/rs13153039, 2021.

Puillat, I., Taupier-Letage, I., and Millot, C.: Algerian eddies lifetime can near 3 years, J. Mar. Syst., 31, 245–259, https://doi.org/10.1016/S0924-7963(01)00056-2, 2002.

Pujol, M.-I., Dupuy, S., Vergara, O., Sánchez-Román, A., Faugère, Y., Prandi, P., Dabat, M.-L., Dagneaux, Q., Lievin, M., Cadier, E., Dibarboure, G., and Picot, N.: Refining the resolution of DUACS along-track (level 3) altimeter sea level products, Earth Syst. Sci. Data, https://doi.org/10.5194/essd-2022-292, 2022.

Rypina, I. I., Pratt, L. J., Entner, S., Anderson, A., and Cherian, D.: The influence of an eddy in the success rates and distributions of passively advected or actively swimming biological organisms crossing the continental slope, J. Phys. Oceanogr., 50, 1839–1852, https://doi.org/10.1175/JPO-D-19-0209.1, 2020.

Schouten, M. W., de Ruijter, W. P. M., van Leeuwen, P. J., and Ridderinkhof, H.: Eddies and variability in the Mozambique Channel, Deep-Sea Res. Pt. II, 50, 1987–2003, https://doi.org/10.1016/S0967-0645(03)00042-0, 2003.

Sutyrin, G. G., Rowe, G. D., Rothstein, L. M., and Ginis, I.: Baroclinic eddy interactions with continental slopes and shelves, J. Phys. Oceanogr., 33, 283–291, https://doi.org/10.1175/1520-0485(2003)033<0283:BEIWCS>2.0.CO;2, 2003.

Testor, P., Send, U., Gascard, J.-C., Millot, C., Taupier-Letage, I., and Béranger, K.: The mean circulation of the southwestern Mediterranean Sea: Algerian Gyres, J. Geophys. Res.-Oceans, 110, C11010, https://doi.org/10.1029/2004JC002861, 2005.

Torres, R., Waldman, R., Mak, J., and Séférian, R.: Global estimation of the eddy kinetic energy dissipation from a diagnostic energy balance, Geophys. Res. Lett., 50, e2023GL104688, https://doi.org/10.1029/2023GL104688, 2023.

Uchoa, I., Simoes-Sousa, I. T., and da Silveira, I. C. A.: The Brazil Current mesoscale eddies: Altimetry-based characterization and tracking, Deep-Sea Res. Pt. I, 192, 103947, https://doi.org/10.1016/j.dsr.2022.103947, 2023.

Verger-Miralles, E., Mourre, B., Gómez-Navarro, L., Barceló-Llull, B., Casas, B., Cutolo, E., et al.: SWOT enhances small-scale eddy detection in the Mediterranean Sea, Geophys. Res. Lett., 52, e2025GL116480, https://doi.org/10.1029/2025GL116480, 2025.

https://doi.org/10.5194/egusphere-2026-3276
Preprint. Discussion started: 24 June 2026


Vignudelli, S., Kostianoy, A. G., Cipollini, P., and Benveniste, J.: Coastal altimetry, Springer, Berlin, Germany, ISBN 978-3-642-12796-0, 2011.

Wang, J., Lucas, A. J., Stalin, S., Lankhorst, M., Send, U., Schofield, O., et al.: SWOT mission validation of sea surface height measurements at sub-100 km scales, Geophys. Res. Lett., 52, e2025GL114936, https://doi.org/10.1029/2025GL114936, 2025.